Subjectively adapted high capacity lossless image data hiding based on prediction errors

M. Fallahpour[1], D. Megias[1], M. Ghanbari[2] (FIEEE)

[1]*Oberta Universidad de Catalunya, Barcelona, Spain*

[2]*School of Computer Science and Electronic Engineering, University of Essex, UK*

MFallahpour@UOC.edu , DMegias@UOC.edu, ghan@essex.ac.uk

Abstract— This article reports on a lossless data hiding scheme for digital images where the data hiding capacity is either determined by minimum acceptable subjective quality or by the demanded capacity. In the proposed method data is hidden within the image prediction errors, where the most well-known prediction algorithms such as the median edge detector (MED), gradient adjacent prediction (GAP) and Jiang prediction are tested for this purpose. In this method, first the histogram of the prediction errors of images are computed and then based on the required capacity or desired image quality, the prediction error values of frequencies larger than this capacity are shifted. The empty space created by such a shift is used for embedding the data. Experimental results show distinct superiority of the image prediction error histogram over the conventional image histogram itself, due to much narrower spectrum of the former over the latter. We have also devised an adaptive method for hiding data, where subjective quality is traded for data hiding capacity. Here the positive and negative error values are chosen such that the sum of their frequencies on the histogram is just above the given capacity or above a certain quality.

Key words: Loss less data hiding; reversible data hiding; image watermarking, prediction

1. Introduction

With the broad use of the Internet and the escalating growth of the information technology, users can easily retrieve multimedia contents with their own computers or mobile phones. Multimedia related researches and applications have extensively increased in the last two decades. Besides multimedia signal processing, data hiding techniques focusing on protecting copyright-related issues are of considerable interest in academia and industry.

Data hiding methods can conceal additional information in media. Most data hiding schemes distort the cover media in order to embed the secret data. Although the distortion is often small and imperceptible, the reversibility is

crucial to some sensitive applications. In applications, such as in law enforcement, medical image systems, it is required to be able to reverse the marked image back to the original cover image for legal consideration. In remote sensing and military imaging, high accuracy is demanded. In some scientific research, experimental data are expensive to be achieved. Under these circumstances, the reversibility of the original media is desired. Reversible data hiding [1,2] is a novel category of data hiding schemes, where at present, there are growing interest in their lossless version.

For the purpose of increasing the embedding capacity, Fridrich et al. [3] presented a new lossless data hiding method based on modifying the least significant bits (LSBs). Their algorithm compresses the least significant bit plane of the cover image and then mixes them alongside the embedded data into the cover image. To improve the data hiding potential of Fridrich et al.'s method, Celik et al. [4] proposed a generalized-LSBs algorithm where the quantization residues of the cover image after the CALIC (context-based adaptive lossless image codec) lossless compression algorithm is used to generate the compressed residues. The remainder of the compression space is used to embed the secret information.

A main category of high-capacity reversible data-embedding algorithms may be classified as expansion-embedding approaches. A common aspect of these approaches is the use of some decorrelating operators to make features with small magnitudes. The data embedding process is done by expanding these features in order to prepare vacancies into which the data bits are embedded. The first algorithm in this category was proposed by Tian [5] and then improved by [6], [7], and [18]. Tian [5] suggested a difference-expansion (DE) scheme that divides the image into pairs of pixels within three groups—expandable, changeable, and nonembeddable—in which information was recorded using a location map. In this method, one hidden bit can be embedded into one of the changeable or expandable pairs. A generalized version of Tian's scheme was enhanced by Alattar [6] to improve the payload, in which instead of pixel pairs the difference expansion of vectors is used. Kamstra et al. [7] have also extended Tian's method by using the information in the low-pass band to find appropriate expandable differences in the high-pass band. Recently Kim et al. [18] improved [5], [7] by introducing a new location map and a new embedding method. Chang et al. [8] suggested a reversible embedding scheme for side match vector quantization

(SMVQ) compressed images. Their scheme can recover only the SMVQ image instead of the vector quantized (VQ) image. Chang and Lin [9] introduced a completely reversible embedding scheme for VQ compressed images. However, the computational cost of their method is high, and it is not suitable for real-time applications.

Following the methods of LSB, difference-expansion and vector quantization algorithm groups, the last category of data hiding reported in [10], [11],[12],[13] and[14] which have attracted great interests in recent years began by the work of Ni et al [10]. The main idea in this category is to use distribution of numbers. These numbers can be the original values of pixels, transformed pixels, etc. Ni et al.[10] introduced a lossless data embedding algorithm based on the spatial domain histogram shifting. An extension to Ni et al work was carried out in [11], where a higher capacity was achieved by relocation of zeros and peaks of the image histogram in image blocks. Recently, Lin and Hsueh [12] presented a reversible method based on increasing the differences between two adjacent pixels. Xuan et al. [13] ,[14] reported a remarkable reversible method where operations are carried out in the integer wavelet transform domain.

Gao et al. [19] use average of differences between pixels of non-overlap image blocks and the block skipping scheme as well as a novel parameter model to guarantee the lossless recovery of the original image. They claim that the method is robust against salt-and-pepper noise and has the potential for capacity adjustment. Algorithm in [20] utilizes a peak point of image histogram and the location map which increases amount of embedding information of [10] at the price of distortion. In [21] a simple and efficient reversible data hiding algorithm is presented which uses the histogram of the differences between sub images obtained through subsampling to enhance [10]. Recently Hong et al. [22] take advantages of median edge detector to design a scheme based on histogram shifting. Tsai et al. [23] with a predictive coding algorithm propose a technique for medical images which improves Ni et al. [10] for some images by about 1.5 dB. However performance of their method is image content dependent and for some images under the same capacity, the quality is poorer than [10].

In these algorithms although through use of prediction, the capacity is improved, but less consideration is paid on the acceptable quality of marked images. What would be more useful, if the capacity could be increased up to the

level that marked image quality is still acceptable. This is what we intend to do in this work, where the embedding capacity is traded for marked image quality.

Our proposed method, named adaptive shifted prediction error (ASPE), is based on hiding data at the locations of larger differences between the pixels of the cover image and their prediction values, to gain from spatial masking of the human visual system. To gain larger masking effect with maximum data hiding capacity, the prediction error at which the number of prediction errors is equal to or larger than the needed capacity is selected to embed the message. Thus one can trade visual quality for the embedding capacity. In this method, the prediction errors larger than the selected error are incremented by “1”. Furthermore, the selected prediction error is left unchanged or incremented by “1” if the embedded bit is “0” or “1”, respectively. Adaptive shifted prediction error (ASPE) method is able to embed a huge amount of data (15-120 kb for a 512 x 512 x 8 grayscale image) while guaranteeing the peak signal-to-noise ratio (PSNR) of the marked image with respect to the original image to be above the perceptual threshold of human visual system (e.g. 40 dB). Moreover, since for the given capacity, the data are hidden at the maximum possible prediction error, then the subjective quality due to special masking is even more impressive. This is because, larger prediction errors do normally occur at edges or highly textured areas of the cover image, where the human visual system is very tolerant to these high spatial frequency distortions (spatial masking). In addition, simplicity, short execution time and applicability to almost all types of images make this method superior to most of the existing reversible data hiding techniques.

The remaining parts of the paper are organized as follows. Section 2 briefly describes most effective pixel prediction strategies. Our proposed algorithm is presented in section 3. Experimental results are given in section 4, with some concluding remarks in section 5.

2. Prediction algorithms

From the literature on prediction techniques, the median edge detector (MED) [15] and the gradient adjusted prediction (GAP) [16] are the states of the art pixel predictors that are used in LOCO-I (Low Complexity Lossless Compression for Images) and CALIC image encoders, respectively. In 2000, Jiang et al. [17]

proposed a predictor that can be thought of as a modified version of MED. For convenience, in this paper, we refer to it the 'Jiang predictor'. In this Section, we briefly introduce the MED, GAP and Jiang predictors. In the following subsections, the pixel to be predicted is denoted by x (the current pixel), and its predicted value chosen by a predictor is denoted by $\hat{x}$. The casual template used in the predictors is shown in Fig. 1, where the shaded area represents the neighboring pixels of the current pixel x that may be used for prediction. For simplicity, *a*, *b*, *c*, *d*, *e*, *f*, *g*, and x also denote both the pixel values and their locations in the figure.

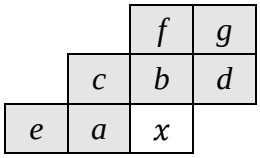

Fig 1. Casual template for pixel prediction

2.1 MED prediction

The MED prediction algorithm is a low-complexity algorithm, operating on three neighbors *a, b* and *c* of the current pixel *x* of the cover image. Applying MED prediction on x , its predicted value $\hat{x}$ is computed according to:

$$\hat{x} = \begin{cases} \min(a,b), & \text{if } c \geq \max(a,b) \\ \max(a,b), & \text{if } c \leq \min(a,b) \\ a+b-c, & \text{otherwise} \end{cases}$$

The MED predictor results in a prediction image with predicted pixel values.

2.2 Gradient adjacent prediction (GAP)

The gradient adjusted prediction algorithm operates on seven neighbors of the current pixel of a cover image x. Applying GAP prediction on x , its predicted value $\hat{x}$ is defined according to the following rules:

$d_h = |a-e| + |b-c| + |b-d|$
$d_v = |a-c| + |b-f| + |d-g|$
if *(* $d_v - d_h > 80$*)* {sharp horizontal edge}
  $\hat{x} = a$
else if *(*$d_v - d_h < -80$*)* {sharp vertical edge}
  $\hat{x} = b$
else *{*
  $\hat{x} = (a+b)/2 + (d-c)/4$ {Smooth area}

if *(* $d_v - d_h$ > 32*)* { horizontal edge}

$\hat{x} = (\hat{x} + a)/2$

if *(* $d_v - d_h$ > 8*)* { weak horizontal edge}

$\hat{x} = (3\hat{x} + a)/4$

if *(* $d_v - d_h$ < – 32*)* { vertical edge}

$\hat{x} = (\hat{x} + b)/2$

if *(* $d_v - d_h$ > 32*)* {weak vertical edge}

$\hat{x} = (3\hat{x} + b)/4$

}

2.3 Jiang prediction

The Jiang predictor in addition to detecting the horizontal and vertical edges as MED does also consider the diagonal edges. This method modifies the conditions c ≥ max(a, *b)* and c ≤ min(a, *b)* of MED asymmetrically. The algorithm of the Jiang predictor is defined as:

if *(* $c \geq \max(a, b)$ *)*
{
  if *(* $c - \max(a, b) > 10$ and $d < b$ and $a - b \geq 5$*)*
    $\hat{x} = (d + \min(a, b))/2$*;*
    else
      $\hat{x} = \min(a, b)$*;*
}
else if *(* $c \leq \min(a, b)$ *)*
  if *(* $10 \leq d - b \leq 50$ *)* and $|b - a| \leq 10$ and $\min(a, b) - c) \geq 5$*))*
    $\hat{x} = (d + \max(a, b))/2$*;*
  else
    $\hat{x} = \max(a, b)$*;*
}
else
  $\hat{x} = a + b - c$*;*

3. Proposed method

Use of histogram of image for data hiding was first proposed by Ni et. al [10]. Then in [11] through image tiling the data hiding capacity was increased. The key point in the histogram based algorithms is the narrower is the histogram the more capacity is available for data hiding. This is because a narrower histogram has a higher peak (as shown in Fig 2) and the positions of the peaks are shifted for maximum capacity of embedding. Hence it is expected the histogram of the prediction error of an image to be able to accommodate more data than the histogram of the image itself. In our adaptive shifted prediction error, ASPE, data

hiding is carried out under two steps of embedding and extraction processes. The embedding process includes selection of the prediction error values according to the required capacity and then shifting the prediction error values according to the rules defined below. The data extraction process is the reverse of data embedding.

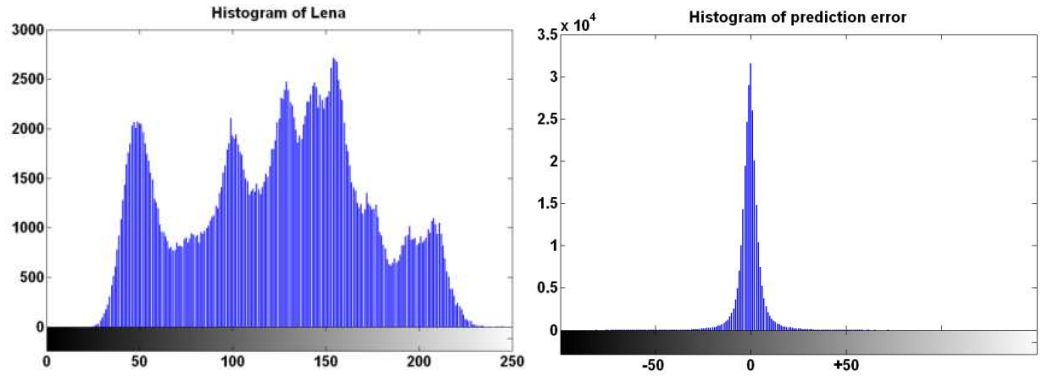

(a) (b)

Fig2. Histogram of Lena (a) image itself (b) prediction error of the image

3.1 Embedding

All kind of lossless predictions can be employed in the ASPE method. Selection of the prediction type depends on the application. For example for real time applications MED may be preferred over GAP because the computational burden and the demanded memory of MED predictor is less than that of GAP. Thus based on the limitations and requirements of the application one can select the most suitable predictor and then the embedding algorithm on this predicted error is as follows:

1) With a chosen prediction algorithm a prediction of the cover image is derived. Steps (2-7) are then performed on this predicted image.
2) The prediction error (PE) matrix elements are calculated by subtracting the predicted image from the cover image, $e_{i,j} = I_{i,j} - \hat{I}_{i,j}$.
3) The number of prediction errors inside the interval [d , d+1) is denoted by D(d). S value is found such that D(S) is equal to or larger than the demanded capacity.
4) To prevent overflow and error in extracting the embedded data, the positions of all pixels with a value of 255 are recorded as side information. Also steps 5 and 6 are carried out for elements with $I_{i,j} < 255$.
5) In the shifting stage, the modified PE matrix is derived from the PE matrix by the following rule: For every $e_{i,j}$ ($(i \neq 1 \; and \; j \neq 1)$ for MED and Jiang predictions, and $(i > 2$ and $j > 2)$ for GAP prediction) if $e_{i,j}$ is equal to or

larger than *S*+1, then the modified PE called $e'_{i,j} = e_{i,j} + 1$, otherwise $e'_{i,j} = e_{i,j}$.

6) In the embedding stage, each $e'_{i,j}$ $((i \neq 1 \text{ and } j \neq 1)$ for MED and Jiang predictions and $(i > 2 \text{ and } j > 2)$ for GAP prediction) with value inside the interval [*S* , *S*+1) is incremented by one if the corresponding bit of the data (to be embedded) is "1", otherwise it will not be modified. After concealing the error data to the modified $e'_{i,j}$, the embedded PE $e''_{i,j}$ is obtained.

7) Finally, the marked image pixel $I_{i,j}{}'$ is reconstructed by $I_{i,j}{}' = \hat{I}_{i,j} + e''_{i,j}$. If $I_{i,j} = 255$ then $I_{i,j}{}' = 255$.

If there are no limits on the computational complexity, payload capacity and image quality of all prediction types are computed and then the best predilection type could be selected. This is due to fact that, depending on image content, one type of prediction may lead to a narrower distribution than the other. Thus with the above embedding steps, the marked pixel $I_{i,j}{}'$ with the embedded bit b_k can be formulated as:

$$I_{i,j}{}' = \begin{cases} \hat{I}_{i,j} + e_{i,j} + 1 & \text{If} \quad e_{i,j} \geq S + 1 \\ \hat{I}_{i,j} + e_{i,j} + b_k & \text{If} \quad e_{i,j} \in [S, S+1) \\ \hat{I}_{i,j} + e_{i,j} & \text{If} \quad e_{i,j} < S \end{cases}$$

Note that, depending on the prediction matrix, not every prediction error can be used for bit embedding. In fact, in MED and Jiang predictions the pixels on the top-most row and the left-most column and for GAP the two top-most rows and the two left-most columns of a cover image are not used for hiding data. To obtain original values of the pixels and the secret information these row/rows and column/columns are reserved and are the same in the cover and marked images. The most right column is not predictable by GAP since for pixels in this column there are no neighbors to *d*, *g*. Thus this column is not useful for embedding secret bits. The gray value of *S*, positions of all pixels with value 255 and prediction type will be treated as side information that need to be transmitted to the receiving end for data retrieval.

The side information could not be embedded in the marked image and they could be transmitted in a secured channel. At the receiver side, this information would be passed through an extractor to recover the hidden data. A second possibility is to introduce a secret key when the side information is required to be embedded

into marked image. This is when a separate channel cannot be provided. In this case, the values should not be embedded as clear text. The bits which form the values must be scrambled using a Pseudo Random Binary Sequence (PRBS) generated through a secret key (seed) and the embedded values would be the result of an XOR sum of the bits of the original values and the bits of the PRBS. The secret key would be also needed at the detector side in order to unscramble the values. Among all possible positions for embedding side information (original or scrambled) LSB bits of the down-most row which are not used for prediction in all three prediction types seem suitable. It is worth noting that data embedding at the encoder and extraction at the decoder follows the raster scan order.

3.2 Detection

The following process is used for extracting the secret message from a marked image and lossless recovery of the cover image with the aid of the side information. Let the marked image pixels $I'_{i,j}$ be the received image at the decoder.

1) As the pixels in the top-most row and left-most column (two top-most rows and two left-most columns in GAP) do not carry any secret data, they can be easily restored by $I_{i,j} = I'_{i,j}$ for i=1 or j=1 (i<3 or j<3 in GAP). Starting from pixel $I'_{2,2}$($I'_{3,3}$ in GAP), the following steps (2-5) are carried out for each pixel completely and then iterated for the next pixel. If $I_{i,j}$ was recorded as side information then $I_{i,j} = I'_{i,j}$ and steps (2-5) are carried out for the next pixel.
2) The predicted pixel $\hat{I}_{i,j}$ of $I_{i,j}$ is reconstructed through the reverse of the prediction algorithm with the pixels that have already been restored.
3) If the embedded PE, $e''_{i,j} = I'_{i,j} - \hat{I}_{i,j}$, is inside the interval [S+1 , S+2), then it is concluded that the embedded data bit was "1". In this case, $e''_{i,j}$ should be decremented by one to obtain the modified PE , $e'_{i,j} = e''_{i,j} - 1$. If $e''_{i,j}$ is inside the interval [S , S+1) the embedded data bit was "0" and $e'_{i,j} = e''_{i,j}$, otherwise there was no embedded data bit and again $e'_{i,j} = e''_{i,j}$. Then to calculate the original prediction error signal, if $e'_{i,j} \geq S$+2 then the prediction error $e_{i,j}$= $e'_{i,j} - 1$, otherwise $e_{i,j} = e'_{i,j}$, where b'_k is the k-th extracted secret bit. The above extracting steps can be formulated as:

$$e_{i,j} = \begin{cases} e''_{i,j} - 1 & \text{If} \quad e''_{i,j} \geq S+2 \\ e''_{i,j} - 1, b'_k = 1 & \text{If} \quad e''_{i,j} \in [S+1, S+2) \\ e''_{i,j}, b'_k = 0 & \text{If} \quad e''_{i,j} \in [S, S+1) \\ e''_{i,j} & \text{If} \quad e''_{i,j} < S \end{cases}$$

4) Finally, $e_{i,j}$ should be added to the prediction value $\hat{I}_{i,j}$ to recover the original cover image pixel, $I_{i,j} = \hat{I}_{i,j} + e_{i,j}$, which is used for the reconstruction of the next pixels.

Fig. 3 shows an example of a 5×5 grey scale image with the GAP prediction. The encoder scans the cover image, Fig. 3(c1), in the raster-scan order pixel by pixel and subtracts the predicted pixels, Fig. 3(c2), from the cover image pixels. Assume the bit stream to be embedded is “010”. In the PE matrix, Fig. 3(c3), the obtained *S* is equal to “0” and D(*S*) = 3. The encoder scans the PE matrix and all elements $(i > 2 \; and \; j > 2)$ equal to or larger than 1 are increased by one, Fig. 3(c4), and then the modified prediction errors in interval [0, 1) are chosen for embedding data. If the corresponding bit of the secret data is ”1”, the modified prediction value is added by one, otherwise it will not be modified, Fig. 3(c5). Marked image, Fig. 3(c6), is obtained by adding the embedded prediction errors, Fig. 3(c5), to the predicted pixels, Fig. 3(c2). It has been already explained that the pixels with $i < 3 \; or \; j < 3$ are the same in the marked and cover images.

The decoder scans the marked image, Fig. 3(d1), starting from the pixel at position (3,3), and does all the steps pixel by pixel with the following rules: Based on the restored cover image pixels, Fig. 3(d2), the prediction pixel value is computed, Fig. 3(d3). If the embedded PE, Fig. 3(d4), is in [0, 1) the embedded data bit will be “0” and the modified PE Fig. 3(d5), is equal to the embedded PE, Fig. 3(d4). If the embedded PE is in [1, 2) the embedded data bit will be “1” and to obtain the modified PE, the embedded PE should be decremented. In case the modified PE is equal to or larger than 2, prediction error, Fig. 3(d6), will be obtained by decrementing the modified PE by one, otherwise PE will be equal to the modified PE. Finally, the restored cover image pixel, Fig. 3(d2), is computed by adding PE to the prediction pixel, Fig. 3(d3).

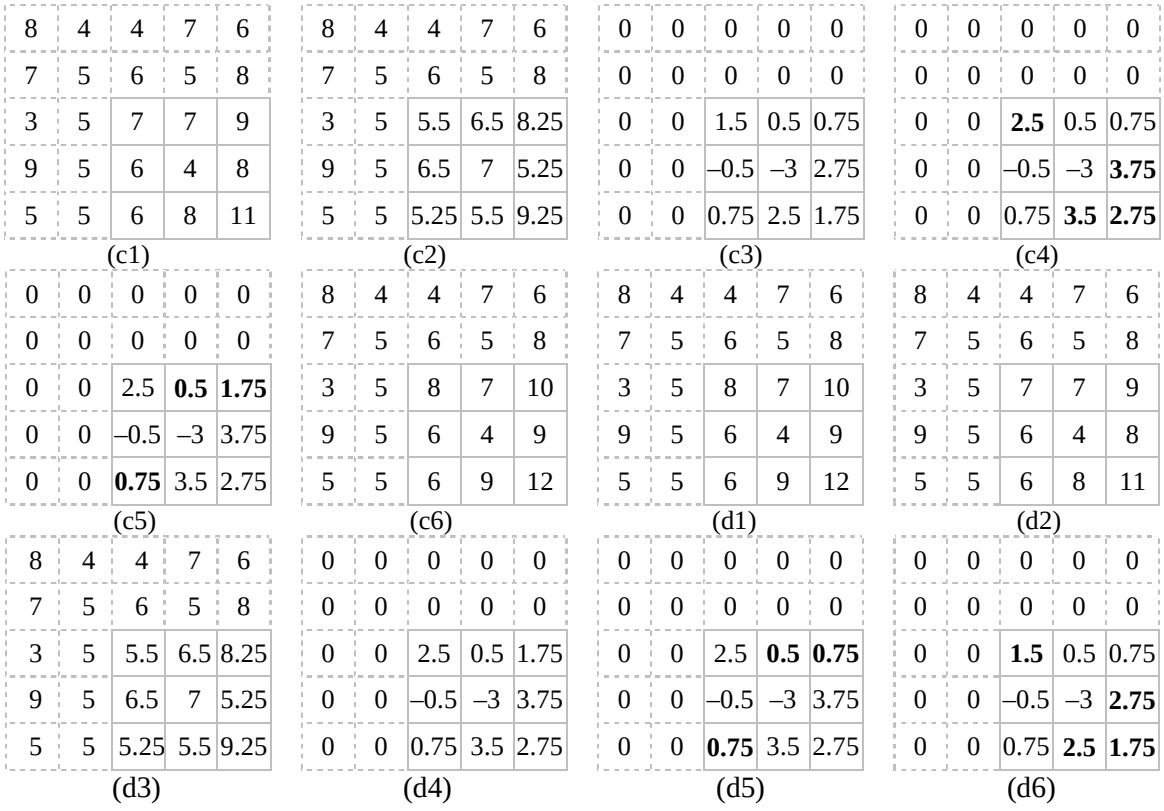

Fig. 3 (c1) – (c6) Embedding steps (d1) – (d6) Detection steps

3.3 Adaptive algorithm

In the shifted histogram based algorithm, the main idea is to create an empty space for the embedding of hidden data. For maximum data hiding capacity, the space belongs to the maximum frequency of the histogram. In fact the narrower the histogram, the more capacity is created. However, when the histogram of the image prediction errors is used, the maximum frequency occurs at zero, as shown in Fig. 4a, which is not suitable for data hiding. This is because, zero valued prediction errors normally occur at the plain areas of pictures, where prediction is more precise and hence the embedded data can be easily perceptible. To alleviate this problem, one may choose the hidden data positions at the textured areas or near the edges of the image, where the human visual masking can be exploited. This is the beauty of the prediction error, where its histogram, unlike the image itself, reflects the image texture and edges. Of course, in this case prediction is not perfect, and also the histogram frequency is not at its maximum, lowering the data hiding capacity. Fortunately, since prediction errors do have an almost symmetric distribution around the maximum frequency, the capacity is twice the frequency

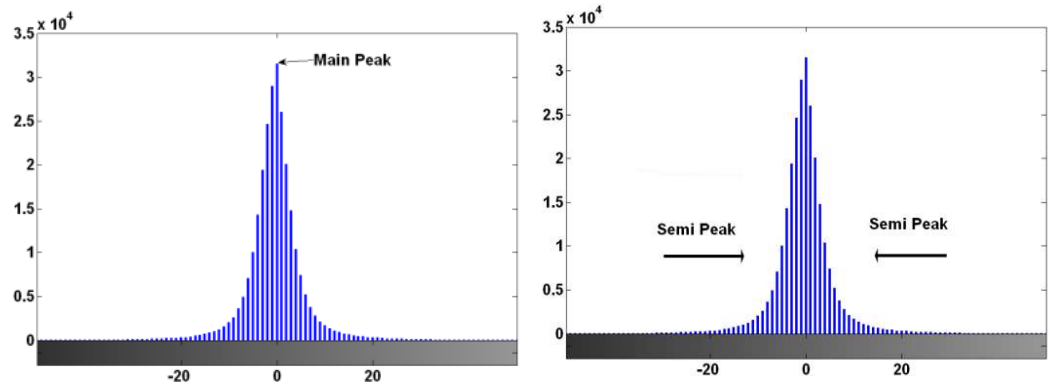

(a) (b)

Fig4. Histogram of prediction error (a) main peak (b) Semi dual-peaks

of the chosen space. Due to this double ended distribution, the sum of positive and negative error frequencies can be even larger than that of frequency at zero.

Fig. 4(a) shows the histogram of the prediction error with the main peak at level zero. The distribution decays towards larger error values where larger prediction errors belong to the textured and edges of the cover image. Thus one can trade the data hiding capacity for the perceived embedding distortion. This means that, the system is capacity/quality adaptive and adaptation is based on choosing positive and negative prediction errors, where their sum of frequencies is just above the given capacity. In practice, we start from both ends of the histogram, from the prediction values of ± 255 towards the origin and when the sum of frequencies is just above the required capacity, the positions of the positive and negative errors are identified for data embedding, as shown in Fig 4(b). It should be born in mind that, since the prediction error might be non-integer, then within the unit interval of [d, d+1), there might exist several prediction errors, whose sum will constitute the frequency in that interval. Here, due to double sided exponential decay of the histogram, as we move towards the origin, the capacity is increased, but since the prediction error due to lower textures is reduced, the distortion becomes more visible.

It should also be noted that the better the prediction strategy, the narrower would be the histogram, increasing the data hiding capacity of the system. Moreover, with good predictors, one can even generate small errors at the highly textured areas. This not only increases the capacity, but also, due to spatial masking at the textured areas, makes them invisible, improving the subjective quality of the marked image.

4. Experimental results and evaluations

Before evaluating the performance of our adaptive shifted prediction error (ASPE) algorithm, let us examine which type of prediction is most suitable for this scheme. Table 1, summarizes the experimental results obtained by using the main peak in ASPE with these three prediction types for Lena, Barbara, Boat, Goldhill, Baboon, Peppers, and Zelda images (512×512×8) of the test images of UWaterloo database[24]. Since the precision of the prediction errors of these prediction types differ, for faire comparison, all error values within a unit interval [*d*, *d*+1), is taken as the representative frequency (cumulative frequency of the unit range) of that interval. With the main peak at the centre, in the Right Shifted type, the created empty space *S* is equal to the prediction error of value "0" and the prediction errors larger than or equal to "1" are incremented by one and the secret bits are embedded in [0,1). In the Left Shifted type the prediction errors smaller than "0" are decremented by one and the embedded bits will be at the prediction errors of [–2,1). Thus, in Right-Left (RL) Shifted type, Right Shifted and Left Shifted types are used simultaneously.

The table shows that RL-shift of all prediction types have almost double the capacity of the right (or left) shift type, indicating the prediction histogram is almost symmetric for all images. Moreover the quality of the marked image in the right shift is almost 3 dB better than in the RL shift. This is due to the fact that, in

Table. 1 PSNR (dB) and payload capacities (bits) of the test images of UWaterloo database[24].

Prediction Type		GAP		Jiang		MED	
Image		Right shift	RL shift	Right shift	RL shift	Right shift	RL shift
Lena	Payload	28971	57949	29624	53963	30031	53836
	PSNR	52.1	49.2	51.3	48.8	51.67	48.68
Barbara	Payload	23816	47363	22554	43477	23005	43995
	PSNR	51.9	49	51.2	48.5	51.59	48.55
Boat	Payload	28941	56850	27454	53275	27883	53313
	PSNR	52.1	49.2	51.2	48.6	51.65	48.63
Goldhill	Payload	20837	41466	20252	39408	20646	40318
	PSNR	52	48.9	51.1	48.5	51.63	48.51
Baboon	Payload	9629	19277	9008	17792	9412	17932
	PSNR	51.5	48.5	51.2	48.3	51.38	48.3
Peppers	Payload	22841	45669	20194	39189	20605	39608
	PSNR	51.9	49	51.2	48.5	51.55	48.51
Zelda	Payload	28906	57908	26016	51039	26434	51347
	PSNR	52.2	49.2	51.2	48.6	51.66	48.61

the right shift almost half of the pixels are unaltered. In general alteration of all pixels by one level (Mean squared error. MSE=1), results in a PSNR of:

$$PSNR = 10\,log_{10}(255 * 255/MSE) = 48.13dB$$

As the table shows all the PSNR of the RL shift are above 48.13 dB, as not all the error pixels are moved and consequently those of Right shift are not less than 51 dB.

It should be noted that the value of prediction error, *d*, also controls the quality and hence the capacity of the embedding system. For example, when d=0, only the whole Right shift elements are displaced by one level, resulting in a PSNR= 51 dB, but for larger d, where values greater than *d* are altered and since the majority of prediction errors are around the centre, then the number of changed pixels is reduced. Our tests for Image Lena, show that for *d*=0, *d*=2, *d*=4 and *d*=6, the PSNR becomes 52.1, 54.7, 57.2 and 59.5 dB respectively. Therefore changing *d*, can also regulate the image quality.

The table also shows that the gradient adjacent prediction has not only larger capacity for data hiding than the other predictors it also has a better quality. The reason is that GAP with seven neighboring pixels uses a better predictor than the other two. Better predictors create smaller prediction errors and hence make the prediction histogram more peaky towards the center. However, its computational complexity is higher than the MED and Jiang predictors. The computation time of GAP is about 4.2 times of MED and 2.2 times of Jiang predictor.

Considering the GAP is the best predictor of all, we now compare the performance of the ASPE with the GAP predictor against the well known high capacity data hiding schemes reported in the literature, such as [5], [7], [10], [11], [12], [13], and [18]. Figure 5 contrasts the performance of ASPE (with the GAP prediction) against these methods for Lena and Barbara images in terms of PSNR and data hiding payload (bpp: bits per pixel). The figure clearly shows the superiority of the ASPE over the other methods. The embedding capacity was limited for a minimum 40 dB in quality. The figure shows that use of more number of *S* the capacity and distortion increase. In generation of data for ASPE, we have used [*d*, *d*+1) for right shift and incremented all errors equal to or larger than *d*+1 to create an empty space in [*d*+1, *d*+2), then the secret bits were embedded in [*d*, *d*+1). For the left shift [–*d*–1, –*d*) was used and the prediction

errors less than $-d$ were decremented to create a vacant space in $[-d-1, -d)$ and then the secret bits were embedded in $[-d-2, -d-1)$. For optimum capacity/distortion, d was chosen as large as possible, and more pairs of d and $-d$ were used to reach the required capacity. i.e. to reach a requested capacity a pair of d and $-d$ is chosen and decrease d to achieve needed capacity. In case if pairs of d=0 do not prepare requested capacity in addition to d=0 another pairs should be selected for embedding which are selected based on needed capacity in a same way. Thus by increasing the number of pairs more capacity can be achieved.

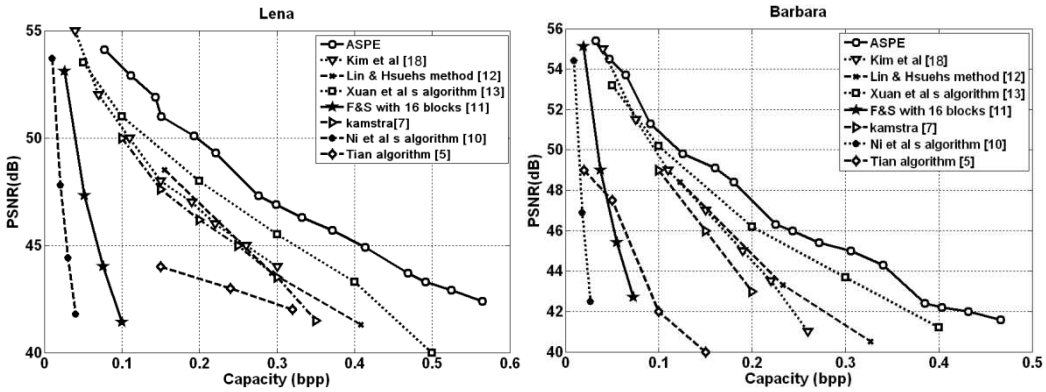

Fig. 5 Comparison among several reversible methods and ASPE for Lena and Barbara images.

One of the main features of our scheme is that the quality of marked image is impaired proportional to the required capacity. However, ASPE has also additional advantage that the rate of decay of impairment is small. To verify this, we implemented this trade off on the Ni et al [10], Hong et al. [22], and Tsai et al. [23] schemes such that frequencies were chosen for the required capacity for Lena and Barbara images, shown in Fig. 6. As the figure shows, while for a capacity of 5 kbits, with Ni et al.[10] PSNR =47.8 dB, and that of ASPE is 59.4 dB, when the capacity is increased to 50 kbits, the quality of the marked image under [10] is dropped below 27 dB, but that of ASPE at this rate is more than 46 dB. However, the PSNR in Hong et al. [22] and Tsai et al. [23] schemes are much better than [10], as shown in Fig. 6, but they are still inferior to ASPE. The main problem with these methods is the lack of efficiency, as both methods suffer the same distortion at 5 and 20 Kbits, which means the data embedding method is not capacity efficient. This is not the case with ASPE and [10], where increasing the capacity the marked image quality degrades accordingly. Moreover the subjective quality of the marked image under ASPE is very good, even at very low PSNRs (the subjective quality of the marked images, do not show any noticeable

distortions to be shown in the paper). As mentioned, the reason for good subjective quality is that, generally histograms of prediction errors do identify the textured and edges and the embedded distortions are masked by them. This is not true for the histogram of the image itself, as used in [10], that cannot exploit the spatial masking property of the human eye. This is in addition to the larger embedding capacity of the former over the latter one.

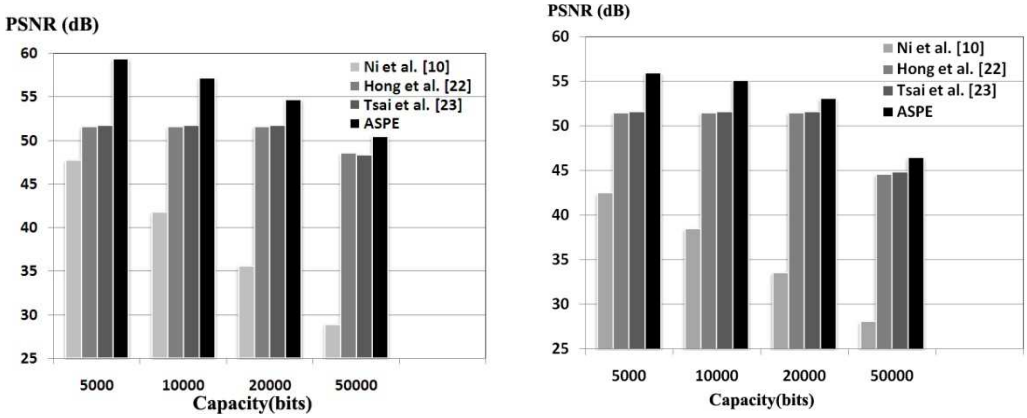

(a)Lena (b) Barbara

Fig.6 Rate of trade off in capacity versus quality between Ni et al [10], Hong et al. [22], Tsai et al. [23] and ASPE.

5. Conclusion

This paper has introduced a high-capacity reversible data hiding algorithm, based on the shifted prediction error histogram. It's ability for adaptively trading capacity for quality, makes sure the highest required capacity is gained at the cost of least quality degradation. Moreover, working on the prediction error histogram, visibility of the hidden data is masked by the texture and edges of the cover image. It was shown that the proposed method outperforms almost all the known reversible data hiding methods and working on pixel differences, the subjective quality of the marked image is even more impressive.

The high capacity of the proposed method is mainly due to the fact that the histograms of predicted error pixels are very peaky. This not only increases the data hiding capacity, but due to narrower density distribution of errors, the marked image is less distorted. Designing of more efficient predictors, particularly better matched to image texture, will undoubtedly improve both the data hiding capacity of the system and the subjectively quality of the marked images.

REFRENCES

1. Y. Q. Shi, Z. Ni, D. Zou, C. Liang, and G. Xuan, “Lossless data hiding: Fundamentals, algorithms and applications,” in *Proc. IEEE Int. Symp. Circuits Syst.*, Vancouver, BC, Canada, vol. II, pp. 33–36, May 2004.

2. J. B. Feng, I. C. Lin, C. S. Tsai, and Y. P. Chu, “Reversible watermarking: current status and key issues,” *International Journal of Network Security*, vol. 2, No. 3, pp. 161-171, May 2006.

3. J. Fridrich, M. Goljan, and R. Du, “Invertible authentication”, in: *Proceedings of SPIE Photonics West, vol. 3971, Security and Watermarking of Multimedia Contents III*, San Jose, CA, pp. 197–208, January 2001.

4. M. U. Celik, G. Sharma, A. M. Tekalp, and E. Saber, “Lossless generalized-LSB data embedding,” *IEEE Trans. Image Process*., vol.14, no.2, pp.253–266, Feb. 2005.

5. J. Tian, “Reversible data embedding using a difference expansion,” *IEEE Trans. Circuits Syst. Video Technol*., vol.13, no.8, pp.890–896, Aug. 2003.

6. A. M. Alattar, “Reversible watermark using the difference expansion of a generalized integer transform,” *IEEE Trans. Image Process.*, vol. 13, no. 8, pp. 1147–1156, Aug. 2004.

7. L. KAMSTRA, and J. A. M. HEIJMANS: ‘Reversible data embedding into images using wavelet techniques and sorting’, *IEEE Trans. Image Process*, 14, (12), pp. 2082–2090, 2005.

8. C.C. CHANG, W. L. TAI, and C.C. LIN: ‘A reversible data hiding scheme based on side match vector quantization’, *IEEE Trans. Circuits Syst. Video Technology.*, 16, (10), pp. 1301–1308, 2006.

9. C. C. CHANG, and C.Y.LIN: ‘Reversible steganography for VQ-compressed images using side matching and relocation’, *IEEE Trans. Inf. Forensics Security*, 1, (4), pp. 493–501,2006.

10. Ni Zhicheng, Y.Q. Shi, N.Ansari, and W. Su, “Reversible data hiding,” *IEEE Trans. on Circuits and Systems for Video technology*, 16(3):354–362, March 2006.

11 M.Fallahpour, M.H. Sedaaghi, "High capacity lossless data hiding based on histogram modification," *IEICE Transactions on Electronics Express* Vol. 4, No. 7 pp.205-210, April 2007.

12 C.C. Lin, and N.L Hsueh, “Hiding Data Reversibly in an Image via Increasing Differences between Two Neighboring Pixels,” *IEICE TRANS. INF. & SYST.*, Vol.E90–D, NO.12 pp 2053-2059, December 2007.

13 G. Xuan, Y. Q. Shi, P. Chai, X. Cui, Z. Ni, and X. Tong, "Optimum Histogram Pair Based Image Lossless Data Embedding," *Proc. International Workshop on DigitalWatermarking (IWDW07)*, Guangzhou, China, 2007.

14 G. Xuan, Y. Q. Shi, C. Yang, Y. Zheng, D. Zou, and P. Chai, “Lossless data hiding using integer wavelet transform and threshold embedding technique,” *IEEE International Conference on Multimedia & Expo (ICME05)*, Amsterdam, Netherlands, July 6-8, 2005.

15 Marcelo J. Weinberger and Gadiel Seroussi “The LOCO-I lossless image compression algorithm: principles and standardization into JPEG-LS*”*, *IEEE Trans. Image Process.* 9 (8) 1309–1324, 2000.

16 X. Wu, and N. Memon, “Context-based, adaptive, lossless image coding”, *IEEE Trans. Commun*. 45 (4) 437–444, 1997.

17 J. Jiang, B. Guo, S. Y. Yang, “Revisiting the JPEG-LS prediction scheme”, *IEE Proc.—Vision, Image Signal Process.* 147 (6) 575–580, 2000.

18 H. J. Kim, V. Sachnev, Y. Q. Shi, J. Nam, and H. G. Choo, “A novel difference expansion transform for reversible data embedding”. *IEEE Trans. Information Forensics and Security*, 3, 3, 456—465, Sep. 2008.

19 X. Gao, L. An, X. Li, D. Tao, “Reversibility improved lossless data hiding” *Signal Processing*, Vol.89, No.10, pp.2053-2065, 2009.

20 J. H. Hwang, J. W. Kim, J. U. CHoi, "A reversible watermarking based on histogram shifting", *LNCS*, Vol. 4283, pp. 348-361, 2006.

21 K. S. Kim, M. J. Lee, H. K. Lee, Y. H. Suh, "Histogram-based reversible data hiding technique using subsampling," Proceedings of the *10th ACM Workshop on Multimedia and Security*, pp. 69-74, 2008.

22 W. Hong, T. S. Chen, C. W. Shiu, "Reversible data hiding based on histogram shifting of prediction errors," Proceedings of the *International Symposium on Intelligent Information Technology Application Workshop*, Vol. 00, No. 292-295, 2008.

23 P. Y. Tsai, Y. C. Hu, H. L. Yeh, "Reversible image hiding scheme using predictive coding and histogram shifting," *Signal Processing*, Vol. 89, No. 6, pp. 1129-1143, 2009.

24 UWaterloo Image Database: http://links.uwaterloo.ca/greyset2.base.html